 MCB, vol.1, no.3, pp.181-190, 2004

An Improved Mathematical Approach for Determination of Molecular Kinetics in Living Cells with FRAP

Tanmay Lele[1], Philmo Oh[1], Jeffrey A. Nickerson[1,2], Donald E. Ingber[1,3]

Abstract: The estimation of binding constants and diffusion coefficients of molecules that associate with insoluble molecular scaffolds inside living cells and nuclei has been facilitated by the use of Fluorescence Recovery after Photobleaching (FRAP) in conjunction with mathematical modeling. A critical feature unique to FRAP experiments that has been overlooked by past mathematical treatments is the existence of an 'equilibrium constraint': local dynamic equilibrium is not disturbed because photobleaching does not functionally destroy molecules, and hence binding-unbinding proceeds at equilibrium rates. Here we describe an improved mathematical formulation under the equilibrium constraint which provides a more accurate estimate of molecular reaction kinetics within FRAP studies carried out in living cells. Due to incorporation of the equilibrium constraint, the original nonlinear kinetic terms become linear allowing for analytical solution of the transport equations and greatly simplifying the estimation process. Based on mathematical modeling and scaling analysis, two experimental measures are identified that can be used to delineate the rate-limiting step. A comprehensive analysis of the interplay between binding-unbinding and diffusion, and its effect on the recovery curve, are presented. This work may help to bring clarity to the study of molecular dynamics within the structural complexity of living cells.

keyword: GFP, cytoskeleton, nuclear matrix, diffusion, mathematical model

[1] Vascular Biology Program, Departments of Pathology and Surgery, Children's Hospital, Harvard Medical School, Boston, MA 02115-5737

[2] Department of Cell Biology and Cancer Center, University of Massachusetts Medical School, North Worcester, MA 01655

[3] Donald Ingber, MD, PhD
Vascular Biology Program
Children's Hospital / Harvard Medical School
Karp Family Research Laboratories, Room 11-127
300 Longwood Ave.
Boston, MA 02115-5737 Ph: 617-919-2223
FAX: 617-730-0230
Email: donald.ingber@childrens.harvard.edu

1 Introduction

Our understanding of cell structure and function is largely based on static images, yet virtually all structures and molecular species are in a state of dynamic equilibrium and undergo continual turnover within living cells. Moreover, it is becoming increasingly clear that many molecules also may become immobilized through binding interactions with insoluble molecular scaffolds, such as signaling complexes, cytoskeletal filaments, and nuclear matrix that appear beneath the surface membrane, in the cytoplasm, and within the nucleus, respectively (Ingber, 1993). A powerful approach for measuring the dynamics of structures and molecules is to track fluorescently tagged molecules in living cells (Lippincott-Schwartz et al., 1999; Lippincott-Schwartz J, 2001). The mobility of molecules (characterized by the diffusion coefficient) can be determined using laser photobleaching techniques, such as fluorescence recovery after photobleaching (FRAP)(Jacobson et al., 1976; Salmon et al., 1984; Schindler et al., 1980) in conjunction with mathematical models (Axelrod et al., 1976; Phair and Misteli, 2001; Tardy et al., 1995). In FRAP, fluorescently-labeled molecules within a small region of the surface membrane, cytoplasm, or nucleus are exposed to a brief pulse of radiation from a laser beam. When the appropriate wavelength of light is utilized, this irradiation bleaches all of the molecules within the path of the beam without altering their structure or function (Phair and Misteli, 2001). Repeated fluorescence images of the bleached zone can be used to measure the rate at which fluorescent molecules redistribute and replace photobleached ones.

If the fluorescent molecules were freely diffusing, then the resulting recovery curve could be used to estimate their diffusion coefficient. However macromolecules in cells usually recover much more slowly than would be predicted for diffusion under similar solution conditions.

This is because many macromolecules in cells are non-covalently bound to insoluble structures in the cytoplasm and nucleus (Ingber, 1993; Penman, 1995), and binding will retard their recovery in FRAP experiments (Nickerson, 2001). Free molecules move at diffusion rates while the bound molecules are relatively immobile. FRAP recovery curves for these molecules are therefore not only a result of diffusion, but rather emerge from the interplay between binding and diffusion. Thus, FRAP data can be potentially employed to make estimates of parameters that characterize the kinetics of molecular interactions inside living cells (Phair and Misteli, 2001). This provides a significant advantage over biochemical methods that study molecules in solution because it permits analysis of the influence of cellular microenvironments on molecular interactions.

The classical mathematical treatment of the FRAP experiment analyzes recovery data by assuming pure diffusion (Axelrod et al., 1976). This theoretical model was initially designed for interpreting the two dimensional recovery of untethered proteins in lipid bilayers. While it was appropriate for this application, it is not well suited for analyzing the recovery of macromolecules that dynamically interact with immobile structures in the nucleus, cytoplasm or cell membranes. However, in the absence of an alternative mathematical treatment, this approach has been used as the method of choice for analysis of FRAP data. Some papers have reported the results of FRAP experiments for cytoskeletal or chromatin proteins as apparent diffusion coefficients, though the authors clearly understood that recovery is limited by binding and not by diffusion. This incongruity which has pervaded the literature resulted from the lack of an alternative, rigorous mathematical treatment of molecular mobility that takes into account both binding and diffusion.

The need for a better interpretation (Nickerson, 2001) and mathematical analysis (Carrero et al., 2003; Kaufman and Jain, 1990; Kaufman and Jain, 1991; Koppel and Sheetz, 1983; Phair and Misteli, 2000; Phair and Misteli, 2001; Presley et al., 2002; Tardy et al., 1995) of FRAP data has been increasingly recognized. Misteli and colleagues have addressed this need by using mathematical modeling to extract binding parameters from FRAP experiments; to accomplish this they assume binding to be the rate-determining step in the recovery (Phair and Misteli, 2000; Phair and Misteli, 2001). Although they modeled the photobleached species, they did not recognize the equilibrium constraint. Others (Tardy et al., 1995) incorporate both binding and diffusion, however, they do not incorporate the photobleached species in their analysis. The equilibrium constraint is based on the fact that the photobleaching process does not destroy molecules of fluorescent species in the photobleached path, but merely makes them invisible (Phair and Misteli, 2001). Assuming that the bound and free molecules were equilibrated with each other before exposure to the laser light, it follows that photobleaching does not disturb this equilibrium in any way. The molecules in the photobleached spot become 'invisible' to the experiment; however their physical presence cannot be ignored.

Here, we incorporate this fact as a key element in a more complete mathematical model. A general theoretical development is presented so that the model can be extended to reaction mechanisms of arbitrary complexity. A comprehensive analysis of the interplay between binding-unbinding and diffusion, and its effect on the recovery curve is also presented. From scaling arguments, analytical expressions are derived for the time of recovery for two scenarios that can potentially exist. We identify two additional measurements during FRAP experiments that can aid in the calculation of binding constants and diffusion coefficients: (1) FRAP analysis of photobleached spots of increasing size, and (2) quantification of the ratio of the bound to free fluorescent molecules at equilibrium. Additionally, the measurement in (1) can provide a rigorous check on the validity of using simplified models, such as those that ignore the effects of diffusion (Phair and Misteli, 2001).

2 Theoretical Considerations

2.1 The Equilibrium Constraint

When significant specific binding occurs to immobile structures inside the irradiated zone, the photobleached molecules in the zone will affect the recovery kinetics of the fluorescent molecules into the spot because they occupy some of the binding sites in this region (Fig. 1). Ignoring this effect does not make a difference when there is no binding to immobile structures, because the equations describing purely diffusive recovery of photobleached and fluorescent molecules are uncoupled. In contrast, when binding to immobile structures occurs, the situation is profoundly different.

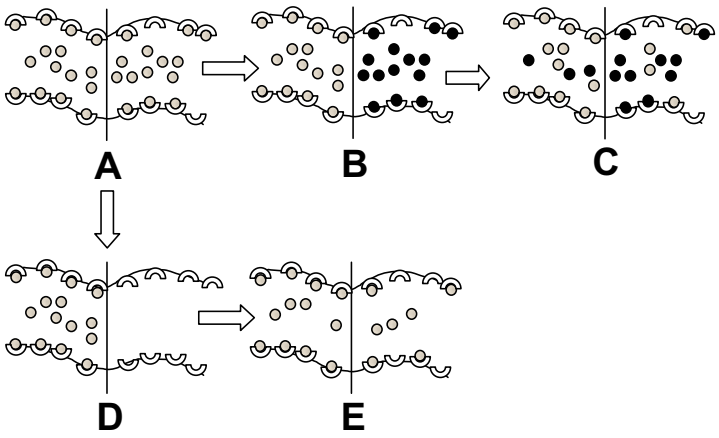

Figure 1 : Diagram of molecular behavior during FRAP and assumptions of current approaches used for FRAP analysis. A) Before photobleaching, the bound molecules are in equilibrium with the free molecules. After photobleaching, there are two different modeling assumptions: B) photobleached molecules are still bound to binding sites or D) these binding sites are assumed to be vacant. These lead to two different scenarios: C) equilibrium binding rates, or E) non-equilibrium binding rates (grey circles, fluorescent molecules; black circles, photobleached molecules).

Consider first the situation in which both free and bound species exist before (Fig. 1A) and after (Fig. 1B) a fraction of the fluorescent molecules has been exposed to fluorescent light. Mobile fluorescent molecules present within adjacent non-irradiated regions will redistribute into the photo-bleached spot by diffusion and then exchange with bound photo-bleached proteins (Fig. 1C). Specifically, they will bind to available binding sites at *equilibrium* binding rates. If one neglects this equilibrium constraint (Fig. 1D), as is done in conventional mathematical models used for analysis of FRAP experiments (Axelrod et al., 1976), the occupied binding sites in the region of interest will be erroneously considered to be vacant; this will give rise to non-equilibrium binding rates (Fig. 1E).

Importantly, the total species concentration always remains constant throughout the FRAP experiment; only the fluorescence intensity of the marker changes. Thus, the mathematical model should be formulated in a manner that ensures that the concentrations of both the fluorescent and photo-bleached molecules *at any time* during the recovery process add up to the initial steady state concentration of fluorescent species. We call this the equilibrium constraint. The equilibrium constraint has profound consequences, as discussed below.

2.2 Formulation of reaction kinetics under the equilibrium constraint

We demonstrate how reaction kinetics should be formulated under the equilibrium constraint. In general, the equilibrium constraint will lead to linear kinetic terms in the model equations. To see this, consider a fluorescent species disappearing with an arbitrary non-linear reaction rate $r(C_0)$ where C_0 is the equilibrium concentration before the photobleaching process. After photobleaching, two species are created, C_F (fluorescent) and C_P (photobleached). Since these two species are absolutely similar except that C_P is optically invisible, the reaction rate at which C_F disappears in the photobleached spot is a fraction of the original reaction rate and is given by $\frac{C_F}{C_F+C_P} r(C_0) = \frac{C_F}{C_0} r(C_0)$. This is clearly linear in C_F. The corresponding rate of disappearance of C_P is $\frac{C_P}{C_0} r(C_0)$. The two rates will add up to the equilibrium reaction rate of $r(C_0)$, which is to be expected since the net reaction rate is unchanged during the experiment.

Thus, the kinetic terms should be formulated such that the equilibrium constraint holds. Specifically, consider a dimerization mechanism where a monomer i disappears with a reaction rate $k_i \left(C_i^0\right)^2$ under equilibrium conditions. After photobleaching, as $C_{i,F}$ enters the photobleached spot, it will dimerize with a constant monomer

concentration of C_i^0 (which are molecules of its own type) without making a distinction between fluorescent or photobleached states. Hence, the rate of disappearance of $C_{i,F}$ will be equal to a fraction $\frac{C_{i,F}}{C_i^0}$ of the equilibrium disappearance rate $k_i \left(C_i^0\right)^2$. Thus the corresponding term in the conservation equation for $C_{i,F}$ is $\frac{C_{i,F}}{C_i^0} k_i \left(C_i^0\right)^2 = k_i C_{i,F} C_i^0$ which is linear in $C_{i,F}$.

3 The Mathematical Model

For illustrative purposes, we model the recovery of fluorescence into a circular photobleached region that is located inside a circular domain (e.g. within the nucleus of a living cell). The mathematical model itself is general and can be applied to FRAP analysis of membranes or cytoplasm as well, provided the geometry of the cell is correctly represented. The size and shape of the nucleus (cell), and associated boundary conditions are important because we model the recovery in a finite domain, unlike the 'infinite' domain assumption in .Axelrod et al. (1976) that has been increasingly challenged in the literature (Carrero et al., 2003; Luby-Phelps, 2000).

3.1 Assumptions in the model

1. We assume that photobleaching is achieved almost uniformly across the irradiated spot in the FRAP experiment. However, the initial photo-bleached profile may be Gaussian owing to the laser intensity being non-uniform across the spot. In that case, this assumption can be easily relaxed (Axelrod et al., 1976).

2. Before photobleaching, the fluorescence is maintained at a constant steady value, i.e. the bound and free molecules are equilibrated with each other. If this is not the case, the model can be extended to time-varying bound and free protein concentrations.

3. The photobleached protein is not functionally destroyed by the photobleaching process (Phair and Misteli, 2001).

4. Both the free and bound molecules are initially uniformly distributed throughout the irradiated domain. If there is a spatial inhomogeneity in the number of binding sites in the domain, this assumption will be invalid (Stenoien et al., 2002; Wagner et al., 2003). We will address such issues in a subsequent publication.

3.2 Model Equations

Let free molecules be denoted by A, and available binding sites by S, then we can denote the binding process by

$$A + S \leftrightarrow AS \tag{1}$$

where AS denotes bound molecules of A. Clearly, the rate of binding will depend not only on the concentration of A, but also on the number of available binding sites S. Without making the distinction between bleached or fluorescent species, we can write down the governing equations for protein transport on the domain Ω (e.g,. the entire nucleus or cell) as:

$$\frac{\partial C}{\partial t} = D\nabla^2 C - k_{ON} C(1 - \frac{\hat{C}}{\tilde{C}_0}) + k_{OFF}\hat{C} \tag{2}$$

$$\frac{\partial \hat{C}}{\partial t} = k_{ON} C(1 - \frac{\hat{C}}{\tilde{C}_0}) - k_{OFF}\hat{C} \tag{3}$$

along with $\nabla C \cdot \mathbf{n} = 0$ on the boundary $\partial\Omega$ (i.e. on the nuclear boundary) which signifies that there is no flux of molecules outside the domain on the time scale of the FRAP experiment. C is the concentration of free species, $\hat{C}$ is the concentration of bound species, $\tilde{C}_0$ is the theoretical concentration that the bound molecules can achieve if bound to all the available binding sites (if there is one bound molecule for every binding site, $\tilde{C}_0$ is the concentration of binding sites), and k_{ON} and k_{OFF} are the rate constants for binding and unbinding, respectively. $(1 - \frac{\hat{C}}{\tilde{C}_0})$ is the fraction of available binding sites (e.g., see the derivation of the Langmuir isotherm; Hiemenz and Rajagopalan, 1997). At steady state, we have:

$$C = C_0 \text{ and } \hat{C}_0 = \frac{k_{ON} C_0 \tilde{C}_0}{k_{ON} C_0 + k_{OFF}\tilde{C}_0} = \frac{C_0 \tilde{C}_0}{C_0 + K\tilde{C}_0} \tag{4}$$

where C_0 and $\hat{C}_0$ are the concentrations of the free and equilibrated bound protein at steady state and $K = \frac{k_{OFF}}{k_{ON}}$ is the equilibrium constant. Thus, before the photobleaching experiment, the free fluorescent species is equilibrated with the bound species and both are uniformly distributed throughout the spot area. Equation 4 can be rearranged to yield

$$\frac{\hat{C}_0}{\tilde{C}_0} = \frac{\gamma}{\gamma + K} \text{ and } \frac{\hat{C}_0}{C_0} = \frac{1}{\gamma + K} \tag{5}$$

where $\gamma \equiv \frac{C_0}{\tilde{C}_0}$ is the ratio of the steady state concentration of free species to the theoretical bound concentration that would be achieved if all binding sites were occupied. Upon photobleaching, there are two optically distinct pools created - photobleached molecules and fluorescent molecules (Fig. 1) - whose concentrations add up to the constant, 'resting' steady state concentration that existed prior to photobleaching. This constraint has to be satisfied at every point in the domain (i.e. not only in the photobleached spot). Let the concentration of photobleached free species be C_P and of fluorescent free species be C_F; similarly that of the bound species will be $\hat{C}_P$ and $\hat{C}_F$. $C_P + C_F = C_0$ and $\hat{C}_P + \hat{C}_F = \hat{C}_0$ are valid throughout the domain, i.e. no gradients are created in the total species concentration; the gradients only exist in the concentrations of the individual bleached and fluorescent molecules. Each of these pools will still obey the conservation equation 2, hence

$$\frac{\partial C_F}{\partial t} = D\nabla^2 C_F - k_{ON} C_F (1 - \frac{\hat{C}_0}{\tilde{C}_0}) + k_{OFF}\hat{C}_F \tag{6}$$

$$\frac{\partial \hat{C}_F}{\partial t} = k_{ON} C_F (1 - \frac{\hat{C}_0}{\tilde{C}_0}) - k_{OFF}\hat{C}_F \tag{7}$$

$$\frac{\partial C_P}{\partial t} = D\nabla^2 C_P - k_{ON} C_P (1 - \frac{\hat{C}_0}{\tilde{C}_0}) + k_{OFF}\hat{C}_P \tag{8}$$

$$\frac{\partial \hat{C}_P}{\partial t} = k_{ON} C_P (1 - \frac{\hat{C}_0}{\tilde{C}_0}) - k_{OFF}\hat{C}_P \tag{9}$$

We stress a very important implication of the above equations. The rate of binding (whether fluorescent or photobleached) is still proportional to the availability of binding sites which is given by $(1 - \frac{\hat{C}_0}{\tilde{C}_0})$. However, since the bound species has equilibrated with the free species before being photobleached, the number of available binding sites is a constant as embodied by the $(1 - \frac{\hat{C}_0}{\tilde{C}_0})$ term. This is a direct consequence of identifying the presence of the photobleached species. If we ignore the photobleached species, then the term would be $(1 - \frac{\hat{C}_F}{\tilde{C}_0})$ and this would allow a very high binding rate in the photobleached region (when $\hat{C}_F = 0$ initially). Equations 6 and 7 are uncoupled from equations 8 and 9 and are linear (even though the original equations were non-linear) and we can solve for the bleached and fluorescent species concentration independently. The zero flux boundary conditions still apply separately to the photobleached and fluorescent species, i.e. $\nabla C_F \cdot \mathbf{n} = \nabla C_P \cdot \mathbf{n} = 0$ on the boundary $\partial\Omega$.

3.3 Scaling

Recovery is a sequential process because the free species has to first diffuse into the spot, and then subsequently exchange with the bound species. The time scale of recovery τ_R will depend on the interplay between binding and unbinding (or reaction) and diffusion. We ignore the situation where k_{ON} is vanishingly small (i.e. $K >> 1$) because then the equilibrium bound concentration $\hat{C}_0 \to 0$ (see equation 5). As a result, there is negligible contribution to the recovery curve by the bound species; and the time scale of recovery would therefore be τ_D. When k_{OFF} is vanishingly small, then $\hat{C}_0 \to \tilde{C}_0$. If $\tilde{C}_0 << C_0$ (i.e. $\gamma >> 1$), then the recovery process is again governed by diffusion because the contribution to the recovery curve by the bound species is negligible. As a result, cases where $\gamma + K >> 1$ can be ignored in the analysis.

The photobleached spot is assumed to be circular with a radius αR (the characteristic length scale) where R is the radius of the entire (circular) domain. This domain for example could correspond to a confocal image of a circular microscopic view within a fluorescent nucleus or cell. We then define the following dimensionless variables: $\xi = \frac{r}{\alpha R}, c_F = \frac{C_F}{C_0}$, $\tau_D \equiv \frac{(\alpha R)^2}{D}$ and $\hat{c}_F = \frac{\hat{C}_F}{\tilde{C}_0}$.

$$\frac{\partial c_F}{\partial \tau} = \nabla^2 c_F - \frac{Da}{\gamma + K}(c_F - \hat{c}_F) \tag{10}$$

$$\frac{\partial \hat{c}_F}{\partial \tau} = Da\,(c_F - \hat{c}_F) \tag{11}$$

where $\nabla^2 \equiv \frac{1}{\xi}\frac{\partial}{\partial \xi}\left(\xi \frac{\partial}{\partial \xi}\right)$. $Da \equiv \frac{k_{OFF}(\alpha R)^2}{D}$ is the Damköhler number (Bird et al., 1960; Deen, 1998) and is the ratio of the characteristic time scale of diffusion to that of binding. The parameter $\gamma + K$ is the ratio of the free species concentration to the bound species concentration at equilibrium (see equation 5)

3.4 Time Scale of Recovery

Case 1:
Binding is Much Faster than Diffusion ($\frac{Da}{\gamma+K} >> 1$)

From equations 12, it is clear that over the time that $\nabla^2 c \sim 1$, $c - c_F \sim \frac{\gamma+K}{Da}$. Thus, $\frac{\partial c}{\partial \tau} \approx \frac{\partial \hat{c}}{\partial \tau}$, and combining equations 12 and 13, we can write

$$\left(1 + \frac{1}{\gamma + K}\right)\frac{\partial c_F}{\partial \tau} = \nabla^2 c_F \tag{12}$$

From (13), the time scale for recovery is

$$\tau_R = \left(\frac{1}{\gamma+K}+1\right)\tau_D = \left(\frac{1}{\gamma+K}+1\right)\frac{\alpha^2 R^2}{D} \tag{13}$$

Case 2:
Binding is Much Slower than Diffusion ($\frac{Da}{\gamma+K} << 1$)

From equations 10 and 11, we see that there are two time scales involved here, one given by τ_D over which $\frac{\partial c_F}{\partial \tau} = \nabla^2 c_F - \frac{Da}{\gamma+K}(c_F - \hat{c}_F) \sim \nabla^2 c_F$, and the other given by τ_{OFF} over which $c_F \sim constant$ and $\frac{1}{Da}\frac{\partial \hat{c}_F}{\partial \tau} = \frac{\partial \hat{c}_F}{k_{OFF}\partial t} = c_F - \hat{c}_F = \text{constant} - \hat{c}_F$.

Thus,

$$\tau_R = \tau_{OFF} = \frac{1}{k_{OFF}} \tag{14}$$

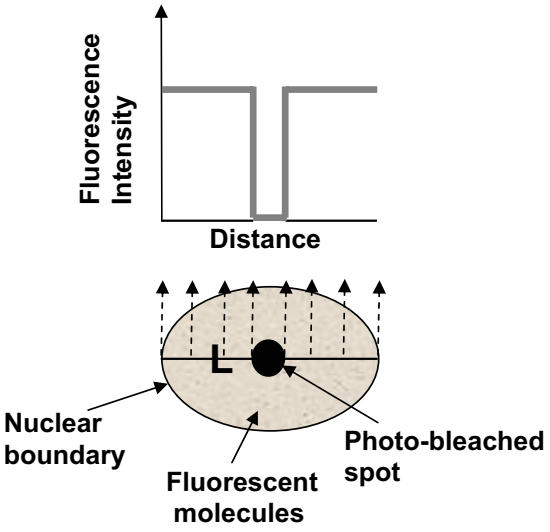

Figure 2 : Schematic of the suggested experimental measurement of fluorescent intensity across a line L drawn across the fluorescent region of interest. The situation immediately after photobleaching is shown where the fluorescent intensity sharply drops off in the photobleached spot.

4 Results and Discussion

In what follows, we will analyze calculations of time-dependent spatial profiles using equations A3 and A4. For illustration, this is shown schematically in Figure 2 where the intensity profile immediately after photobleaching is shown along line L. As recovery proceeds, the spatial profile across the photobleached region of interest would change with time finally achieving a spatially homogeneous constant value at the end of recovery. The measured fluorescence intensity is the sum of free as well as bound protein. These contributions cannot be measured separately during the FRAP experiment and hence we analyze them below.

For significant contribution by the bound species to the recovery curve, $k_{OFF} \leq k_{ON}$, i.e. the equilibrium concentration of bound species should be comparable to the free species concentration. The discussion below is based on this assumption. The fluorescence recovery in the photobleached spot is a sequential process in which the free species first diffuses into the irradiated region and then binds to available immobile binding sites. The ratio of the time scales governing these two processes (expressed by the dimensionless parameter $\frac{Da}{\gamma+K}$) decides the rate-determining step. If $\frac{Da}{\gamma+K} << 1$; the recovery process is limited by the kinetics of binding-unbinding. This results in rapid recovery of the free species in the photobleached spot, followed by a slow recovery of bound species as seen in Fig. 3A (which is obtained by plotting the analytical solution presented in equations A3 and A4 in the Appendix). Owing to fast diffusion, any spatial gradients are almost homogenized. The total recovery curve is due to a weighted sum of these two profiles and would therefore be devoid of any spatial gradients as well (Fig. 3A). This implies that the free species achieves a nearly spatially homogenous dimensionless value of $1-\alpha^2$throughout the recovery process. In such a case, the rate of the overall recovery process will be governed by k_{OFF} (also see the discussion on time scale analysis (for Case 2). Then the equations 9 and 10 can be approximated as $\frac{d\hat{c}_F}{d\omega} = c_F - \hat{c}_F = 1-\alpha^2 - \hat{c}_F$ with an initial condition $\hat{c}_F(0) = 0$ in the photobleached spot. This equation can be easily integrated and k_{OFF} can be estimated by fitting the resulting spatially averaged solution to the measured recovery curve.

Thus, if reaction kinetics are the rate governing step, mathematical models may be simplified into a system of ordinary differential equations. This is particularly useful when there are multiple interacting species involved (Phair and Misteli, 2000; Phair and Misteli, 2001), and it makes the estimation process simpler especially for non-linear models. However, it is important to experimentally measure and confirm this. To accomplish this, we sug-

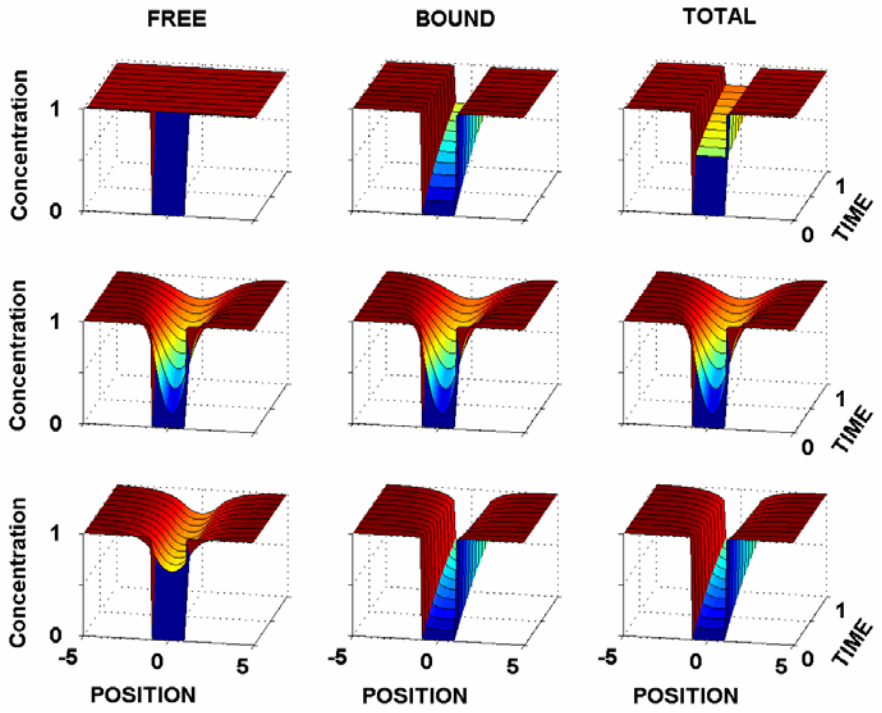

Figure 3 : Time-dependent spatial profiles of fluorescence recovery in the line L across the photobleached spot of the free, bound and total normalized species concentrations (all variables are dimensionless as defined in the text and is used for the time scale, see equations 14 and 15). $C_0 = 1$ nM (initial free concentration), $\alpha = 0.2$ (ratio of spot to nuclear radius). A) The case in which diffusion is much faster than binding and unbinding ($\frac{Da}{\gamma+K} = 0.001$, $Da = 0.001$). The free species recovers quickly followed by slow recovery of bound species, and hence no spatial gradients exist. B) The case in which diffusion is exactly as fast as unbinding but much slower than binding ($\frac{Da}{\gamma+K} = 1000, \gamma+K = 0.001$). The free and bound species recover as if in equilibrium owing to the high binding rates. Thus, as the free species recovers via diffusion, spatial gradients in its concentration are mirrored in the bound species concentration, resulting in gradients in the total species profile. C) The case in which unbinding is slower than diffusion which is exactly as fast as binding ($\frac{Da}{\gamma+K} = 1, \gamma+K = 0.01$). The free species recovers but not completely; this results in minor spatial gradients in the total concentration.

gest FRAP analysis of photobleached spots of increasing size. If the process is diffusion limited, the recovery time wil scale as the square of the size of the photobleached spot (equation 13). If there is no size dependence at all, then the process is governed by reaction kinetics.

When there is significantly slower recovery of fluorescence (on the order of minutes), it is tempting to assume that k_{OFF} (i.e. the unbinding rate of fluorescent molecules) is very small and thereby governs the time scale of recovery. It is generally assumed that this could not be a result of purely slow diffusion because pure diffusion of most molecules is relatively fast, with some of the slowest moving molecules recovering under less than a minute. However, there is an alternate explanation for reduced mobility, as described below.

Let $\frac{Da}{\gamma+K} >> 1$, i.e. diffusion is slower than binding. Let us assume that the initial equilibrium concentration of bound species is significantly large compared to the free species, as seen, for example, in fluorescent splicing speckles or protein localizations in FRAP studies of the nucleus (Stenoien et al., 2002; Wagner et al., 2003). This implies that $\gamma+K << 1$, i.e. binding is much faster than unbinding so that $\tau_{ON} << \tau_{OFF}$ and the concentration of binding sites is much higher than the free species concentration so that $\gamma << 1$. Let us assume that diffusion is exactly as fast as unbinding (i.e. $\tau_D = \tau_{OFF}$ so that $Da = 1$). Then, the time of recovery is equal to the time required for diffusive transport via a small

number of free species molecules to replenish the large number of bound photobleached molecules (this follows from scaling arguments as shown above). In other words, owing to the large excess of bound protein over free protein, it takes more time for the recovery to occur, which is given by $\tau_R = \left(\frac{1}{\gamma+K}+1\right)\frac{\alpha^2R^2}{D}$ (see equation 14). For $\gamma+K=0.001$, and $\tau_D=\tau_{OFF}=1$ second, $\tau_R=1000$ seconds. Clearly, it would be erroneous to presuppose that slow recovery is necessarily due to slow unbinding, as assumed in past models (Phair and Misteli, 2000; Phair and Misteli, 2001). In fact, in this case, the time of recovery does not depend on k_{OFF} at all, but rather on $\gamma+K$, the ratio of initial free to bound concentration of fluorescent species. In this situation, a strong spatial dependence in the net profile will exist along a line drawn across the photobleached spot throughout the time course of the recovery curve (Fig. 3 B versus 3A). The process can be conceptualized as a purely diffusive process but with an effective diffusion coefficient given by $D_{eff} = \frac{D}{\left(\frac{1}{\gamma+K}+1\right)}$ which is much lower than D.

There are other scenarios in addition to the one discussed above which could be potentially applicable. For the case where $\gamma+K << 1$ and $\frac{Da}{\gamma+K} \sim 1$ which implies that diffusion is comparable to the rate of binding, small spatial gradients will arise . There will be quick but incomplete initial recovery of the free species that will cause the gradients to become shallower, followed by a slow recovery in the bound species concentration (Fig. 3C). While the various possibilities depending on $\gamma+K$ are too numerous to go into here, they all fall into two basic categories, given by $\frac{Da}{\gamma+K} < 1$ or $\frac{Da}{\gamma+K} \geq 1$.

The analytical solution for the recovery curve (equation A7 in Appendix) encompasses all of the above possibilities and can therefore be used to calculate binding constants and diffusion coefficients for any of the above situations. The parameters that will be estimated are Da, the Damköhler number, which is a ratio of the time scales of diffusion and binding, τ_D, the time scale for diffusion and $\gamma+K$, the ratio of the equilibrium free to bound concentration. Any standard non-linear least squares fitting algorithm can be used. Since this is a multi-parameter, non-linear estimation, initial guesses for the parameters are invaluable in helping the fitting algorithm to converge. Two measurements can prove useful. One is to measure the ratio of free to bound species concentration that will directly yield $\gamma+K$. Then, the parameters that are left to be estimated are Da and τ_D. By photobleaching spots of increasing size, one can check if the time of recovery scales as given by equation (13). If the measured τ_R is insensitive to size, then the process is governed entirely by reaction kinetics (the time of recovery τ_R is available directly from the recovery curve) and the initial guess is $Da < \gamma+K$ and $\tau_{OFF}=\tau_R$. If there is a dependence on the size of the photobleached spot, the starting initial guesses are $Da > \gamma+K$ and $\tau_D = (\gamma+K)\tau_R$. These provide reasonable initial guesses to fitting algorithms and therefore help them to converge. Once Da and τ_D are known, $D = \frac{(\alpha R)^2}{\tau_D}$ and $k_{OFF} = \frac{Da}{\tau_D}$.

In conclusion, molecular binding parameters measured with FRAP often are a result of interplay between diffusion and molecular interactions with binding sites on immobile structures when they are present inside living cells.Because FRAP does not disrupt the local equilibrium, the equations that describe recovery should be formulated under an equilibrium constraint. Two additional experimental measurements - the equilibrium concentrations of bound and free species and FRAP of increasing spot sizes to identify the rate determining step - are suggested which can potentially aid in the accurate estimation of kinetic parameters from recovery data. In the case of slow fluorescence recovery, a slow unbinding rate (i.e. small k_{OFF}) represents only one of many possibilities that exist to explain this behavior. Hence, instead of using simplified kinetic models for the estimation of these parameters, a rigorous solution that describes the influence of diffusion on the recovery curve should be utilized; a solution of this type is presented in equation A7. For a large number of interacting species, the resulting linear system of partial differential equations (equation 18) can be analytically solved using linear operator techniques; the solution methodology is available in .Ramkrishna and Amundson (1985). On the other hand, if reaction kinetics is found to be rate limiting, appropriate model simplification can be done which is particularly useful when a large number of interacting species are involved and the kinetic rate laws are non-linear. This mathematical treatment of FRAP will hopefully help to bring clarity to the study of the dynamics of molecules that exist within both soluble and immobilized forms within living cells.

Acknowledgement: This work was supported by grants from NASA (NAG2-1501), NIH (CA-45548), and

by the NSF-funded Materials Research Science and Engineering Center (MRSEC) of Harvard University.

References

Axelrod, D.; Koppel, D.; Schlessinger, J.; Elson, E.; Webb, W. (1976): Mobility measurement by analysis of fluorescence photobleaching recovery kinetics. *Biophys J*. 16:1055-69.

Bird, B.; Steward, W.; Lightfood, E. (1960): Transport Phenomena. John Wiley and Sons, New York.

Carrero, G.; McDonald, D.; Crawford, E.; de Vries, G.; Hendzel, M. (2003): Using FRAP and mathematical modeling to determine the in vivo kinetics of nuclear proteins. *Methods*. 29:14-28.

Deen, W. (1998): Analysis of Transport Phenomena. Oxford University Press.

Hiemenz, P. C.; Rajagopalan, R. (1997): Principles of Colloid and Surface Chemistry. Marcel Dekker.

Ingber, D. E. (1993): The riddle of morphogenesis: a question of solution chemistry or molecular cell engineering? *Cell*. 75:1249-52.

Jacobson, K.; Derzko, Z.; Wu, E. S.; Hou, Y.; Poste, G. (1976): Measurement of the lateral mobility of cell surface components in single, living cells by fluorescence recovery after photobleaching. *J Supramol Struct*. 5:565(417)-576(428).

Kaufman, E. N.; Jain, R. K. (1990): Quantification of transport and binding parameters using Fluorescence Recovery after Photobleaching. *Biophys J*. 58:873-885.

Kaufman, E. N.; Jain, R. K. (1991): Measurement of mass transport and reaction parameters in bulk solution using photobleaching. *Biophys J*. 60:596-608.

Koppel, D.; Sheetz, M. (1983): A localized pattern photobleaching method for the concurrent analysis of rapid and slow diffusion processes. *Biophys J*. 43:175-181.

Lippincott-Schwartz, J.; Presley, J.; Zaal, K.; Hirschberg, K.; Miller, C.; Ellenberg, J. (1999): Monitoring the dynamics and mobility of membrane proteins tagged with green fluorescent protein. *Methods Cell Biol*. 58:261-81.

Lippincott-Schwartz, J.; S. E.; Kenworthy, A. (2001): Studying protein dynamics in living cells. *Nat Rev Mol Cell Biol*. 2:444-56.

Luby-Phelps, K. (2000): Cytoarchitecture and physical properties of cytoplasm: volume, viscosity, diffusion, intracellular surface area. *Int Rev Cytol*. 192:189-221.

Nickerson, J. (2001): Experimental observations of a nuclear matrix. *J Cell Sci*. 114:463-74.

Penman, S. (1995): Rethinking cell structure. *Proc Natl Acad Sci U S A*. 92:5251-7.

Phair, R.; Misteli, T. (2000): High mobility of proteins in the mammalian cell nucleus. *Nature*. 404:604-9.

Phair, R.; Misteli, T. (2001): Kinetic modelling approaches to in vivo imaging. *Nat Rev Mol Cell Biol*. 2:898-907.

Presley, J.; Ward, T.; Pfeifer, A.; Siggia, E.; Phair, R.; Lippincott-Schwartz, J. (2002): Dissection of COPI and Arf1 dynamics in vivo and role in Golgi membrane transport. *Nature*. 417:187-93.

Ramkrishna, D.; Amundson, N. (1985): Linear operator methods in chemical engineering with applications to transport and chemical reaction systems. Prentice-Hall, Englewood Cliffs,NJ.

Salmon, E. D.; Leslie, R. J.; Saxton, W. M.; Karow, M. L.; McIntosh, J. R. (1984): Spindle microtubule dynamics in sea urchin embryos: analysis using a fluorescein-labeled tubulin and measurements of fluorescence redistribution after laser photobleaching. *J Cell Biol*. 99:2165-74.

Schindler, M.; Osborn, M. J.; Koppel, D. E. (1980): Lateral diffusion of lipopolysaccharide in the outer membrane of Salmonella typhimurium. *Nature*. 285:261-3.

Stenoien, D.; Mielke, M.; Mancini, M. (2002): Intranuclear ataxin1 inclusions contain both fast- and slow-exchanging components. *Nat Cell Biol*. 4:806-10.

Tardy, Y.; McGrath, J.; Hartwig, J.; Dewey, C. (1995): Interpreting Photoactivated Fluorescence Microscopy Measurements of Steady-State Actin Dynamics. *Biophys J*. 69:1674-1682.

Wagner, S.; Chiosea, S.; Nickerson, J. (2003): The spatial targeting and nuclear matrix binding domains of SRm160. *Proc Natl Acad Sci*. 100:3269-74.

Appendix

Here, we solve the full system of equations for the general case. Equations 11 and 12 that describe the recovery

process are reproduced here:

$$\frac{\partial c_F}{\partial \tau} = \nabla^2 c_F - \frac{Da}{\gamma+K}(c_F - \hat{c}_F) \tag{A1}$$

$$\frac{\partial \hat{c}_F}{\partial \tau} = Da\,(c_F - \hat{c}_F) \tag{A2}$$

where $\nabla^2 \equiv \frac{1}{\xi}\frac{\partial}{\partial \xi}\left(\xi \frac{\partial}{\partial \xi}\right)$. The equations are subject to boundary conditions $\nabla c_F \cdot \mathbf{n} = \nabla \hat{c}_F \cdot \mathbf{n} = 0$ at $\xi = 0$ and $\xi = {}^{1}/_{\alpha}$. The initial condition is $c_F(0,\xi) = \hat{c}_F(0,\xi) = H(\xi - 1)$. Since $\hat{c}_F$ is immobile, its dependence on ξ is derived from that of c_F. Hence, the eigenfunctions in the expansion of $\hat{c}_F$ and c_F are identical. We can write the solution as $c_F = \sum_{n=0}^{\infty} \Phi_n(\xi) c_n(\tau)$ and $\hat{c}_F = \sum_{n=0}^{\infty} \Phi_n(\xi)\hat{c}_n(\tau)$ where $\Phi_0(\xi) = \sqrt{2}\alpha$ and $\Phi_n(\xi) = \sqrt{2}\alpha \frac{J_0(\lambda_n \xi)}{J_0\left({}^{\lambda_n}/_{\alpha}\right)}$, $n = 1,2,..,$ where λ_n is given by the solution of $J_1\left({}^{\lambda_n}/_{\alpha}\right) = 0$ (see (Deen, 1998)). Thus,

$$c_F(\tau,\xi) = \sqrt{2}\alpha c_0(\tau) + \sum_{n=1}^{\infty} \sqrt{2}\alpha \frac{J_0(\lambda_n \xi)}{J_0\left({}^{\lambda_n}/_{\alpha}\right)} c_n(\tau) \tag{A3}$$

and

$$\hat{c}_F(\tau,\xi) = \sqrt{2}\alpha c_0(\tau) + \sum_{n=1}^{\infty} \sqrt{2}\alpha \frac{J_0(\lambda_n \xi)}{J_0\left({}^{\lambda_n}/_{\alpha}\right)} \hat{c}_n(\tau) \tag{A4}$$

Then, the transformed concentrations can be written as $c_n(\tau) = \int_0^{1/\alpha} \Phi_n(\xi)\, c(\xi,\tau)\, \xi d\xi$ and $\hat{c}_n(\tau) = \int_0^{1/\alpha} \Phi_n(\xi)\, \hat{c}(\xi,\tau)\, \xi d\xi$. Transforming equations A1 and A2 above, we get

$$\frac{dc_0}{d\tau} = -\frac{Da}{\gamma+K} c_0 + \frac{Da}{\gamma+K}\hat{c}_0, \quad \frac{d\hat{c}_0}{d\tau} = Da\,(c_0 - \hat{c}_0) \tag{A5}$$

$$\frac{dc_n}{d\tau} = -\left(\lambda_n^2 + \frac{Da}{\gamma+K}\right) c_n + \frac{Da}{\gamma+K}\hat{c}_n,$$
$$\frac{d\hat{c}_n}{d\tau} = Da\,(c_n - \hat{c}_n), n = 1,2,... \tag{A6}$$

The initial condition is transformed to yield $c_0 = \hat{c}_0 = \frac{\alpha}{\sqrt{2}}\left(\frac{1}{\alpha^2} - 1\right)$ and $c_n(0) = \hat{c}_n(0) = -\frac{\sqrt{2}\alpha J_1(\lambda_n)}{\lambda_n J_0\left({}^{\lambda_n}/_{\alpha}\right)}$. The equations A5 and A6 along with initial conditions can easily analytically solved; substitution of the resulting solution into (A4) and (A4) yields the solution to (A1) and (A2).

The recovery curve normalized to the *initial* amount of fluorescent species is given by:

$$\int_0^1 \frac{\left(c_F C_0 + \hat{c}_F \hat{C}_0\right)}{\frac{C_0+\hat{C}_0}{2}} \xi d\xi$$
$$= 2\int_0^1 \left(\frac{(\gamma+K)\,c_F}{\gamma+K+1} + \frac{\hat{c}_F}{\gamma+K+1}\right)\xi d\xi$$
$$= \frac{2}{\gamma+K+1}\int_0^1 \left((\gamma+K)\,c_F + \hat{c}_F\right)\xi d\xi$$
$$= \frac{2}{\gamma+K+1}\sum_{n=0}^{\infty}\left((\gamma+K)\,c_n(\tau) + \hat{c}_n(\tau)\right)\int_0^1 \Phi_n(\xi)\,\xi d\xi$$
$$= \frac{2\sqrt{2}\alpha}{\gamma+K+1}\left(\left((\gamma+K)\,c_0(\tau) + \hat{c}_0(\tau)\right)\int_0^1 \xi d\xi + \sum_{n=1}^{\infty}\frac{\left((\gamma+K)\,c_n(\tau) + \hat{c}_n(\tau)\right)}{J_0\left({}^{\lambda_n}/_{\alpha}\right)}\int_0^1 J_0(\lambda_n\xi)\,\xi d\xi\right)$$
$$= \frac{2\sqrt{2}\alpha}{(\gamma+K+1)}\left(\frac{(\gamma+K)\,c_0(\tau) + \hat{c}_0(\tau)}{2} + \sum_{n=0}^{\infty}\frac{\left((\gamma+K)\,c_n(\tau) + \hat{c}_n(\tau)\right)J_1(\lambda_n)}{\lambda_n J_0\left({}^{\lambda_n}/_{\alpha}\right)}\right)$$

Thus, the recovery curve normalized to the initial amount of fluorescence is

$$f(\tau) = \frac{2\sqrt{2}\alpha}{(\gamma+K+1)}\left(\frac{(\gamma+K)\,c_0(\tau) + \hat{c}_0(\tau)}{2} + \sum_{n=0}^{\infty}\frac{\left((\gamma+K)\,c_n(\tau) + \hat{c}_n(\tau)\right)J_1(\lambda_n)}{\lambda_n J_0\left({}^{\lambda_n}/_{\alpha}\right)}\right) \tag{A7}$$